



# Stability of milk-derived calcium phosphate suspensions

Skelte G. Anema

## ► To cite this version:

Skelte G. Anema. Stability of milk-derived calcium phosphate suspensions. Dairy Science & Technology, 2009, 89 (3-4), pp.269-282. hal-00895798

**HAL Id: hal-00895798**

**<https://hal.science/hal-00895798>**

Submitted on 11 May 2020

**HAL** is a multi-disciplinary open access archive for the deposit and dissemination of scientific research documents, whether they are published or not. The documents may come from teaching and research institutions in France or abroad, or from public or private research centers.

L'archive ouverte pluridisciplinaire **HAL**, est destinée au dépôt et à la diffusion de documents scientifiques de niveau recherche, publiés ou non, émanant des établissements d'enseignement et de recherche français ou étrangers, des laboratoires publics ou privés.

# Stability of milk-derived calcium phosphate suspensions

Skelte G. ANEMA\*

Fonterra Research Centre, Private Bag 11029, Palmerston North, New Zealand

Received 24 September 2008 – Accepted 22 January 2009

**Abstract** – Milk-derived calcium phosphate (MDCP) can be isolated from whey derived from acid casein or cottage cheese manufacture as a precipitated calcium phosphate material. However, the composition and suspension properties of this MDCP material are poorly understood. This study was aimed at examining the properties of MDCP when in suspension, and the factors affecting the stability of this calcium phosphate suspension. When suspended in water, MDCP aggregated, with the aggregation rate increasing with increasing temperature. Aggregation was more rapid in milk permeate than in water. The aggregation of MDCP increased with increasing ionic strength, and, as this was accompanied by a decrease in the magnitude of the  $\zeta$ -potential, this could be explained by the effects of the electrolyte concentrations on the electrical double layers of the particles. Soluble calcium markedly increased the rate of aggregation of the MDCP, whereas soluble phosphate slightly retarded the aggregation. Soluble calcium changed the  $\zeta$ -potential from negative to positive, with the particles becoming progressively more positive at higher soluble calcium levels. In contrast, increasing soluble phosphate levels made the  $\zeta$ -potential of MDCP particles markedly more negative. These results indicate that the addition of soluble calcium or soluble phosphate had more specific effects, probably binding to the surface of the MDCP particles. The increased rate of aggregation in soluble calcium solutions could not be solely explained by the changes to the  $\zeta$ -potentials of the particles.

**milk / calcium / phosphate / aggregation /  $\zeta$ -potential / ionic strength**

**摘要** – 乳源磷酸钙悬浮液的稳定性。乳源磷酸钙 (MDCP) 是从酸沉酪蛋白或者生产软干酪的乳清中制备的磷酸钙沉淀物。目前关于 MDCP 的组成和悬浮液性质知之甚少。本文研究了 MDCP 悬浮液的特性和影响这种悬浮液稳定的因素。当将 MDCP 悬浮在水中时, MDCP 发生凝聚, 而且随着温度的增加, MDCP 的凝聚速度增加。这种凝聚速度在乳超滤透过液中比在纯水中快。随着溶液离子强度的增加 MDCP 的凝聚作用增加, 并且伴随着  $\zeta$ -电势大幅度的降低, 这种现象可以解释为由于粒子双电层电解液浓缩作用的影响。可溶性钙可以显著地增加 MDCP 的凝聚速率, 而可溶性磷酸盐可以略微延迟凝聚作用。可溶性钙使 MDCP 粒子的  $\zeta$ -电势从负值到正值, 而且随着可溶性钙浓度的增加  $\zeta$ -电势的正值越大。相反, 增加可溶性磷酸盐浓度, 使得 MDCP 粒子的  $\zeta$ -电势降到更低的负值。试验结果表明添加可溶性钙和可溶性磷酸盐对 MDCP 产生了独特的影响, 可能是由于它们束缚在 MDCP 粒子表面的原因。仅用粒子表面  $\zeta$ -电势的变化还不能充分解释在可溶性钙溶液中 MDCP 凝聚速率增加的原因。

**乳 / 钙 / 磷酸盐 / 凝聚作用 /  $\zeta$ -电势 / 离子强度**

\*Corresponding author (通讯作者): [skelte.anema@fonterra.com](mailto:skelte.anema@fonterra.com)

**Résumé – Stabilité de suspensions de phosphate de calcium dérivé de lait.** Du phosphate de calcium d'origine laitière (PCL) peut être isolé à partir de lactosérum provenant de la fabrication de caséine acide ou de fromage Cottage sous forme de phosphate de calcium précipité. Cependant, la composition et les propriétés de suspension de ce PCL sont peu connues. Le but de cette étude était d'examiner les propriétés du PCL en suspension et les facteurs affectant la stabilité de cette suspension de phosphate de calcium. En suspension dans l'eau, le PCL s'agrégeait, et ce, d'autant plus que la température augmentait. L'agrégation était plus rapide dans le perméat de lait que dans l'eau. L'agrégation de PCL augmentait quand la force ionique augmentait, et, comme ceci s'accompagnait d'une diminution de magnitude du potentiel zeta, ce phénomène pourrait s'expliquer par les effets des concentrations en électrolyte sur les doubles couches électriques des particules. Le calcium soluble augmentait nettement le taux d'agrégation du PCL alors que le phosphate soluble retardait légèrement l'agrégation. Le calcium soluble faisait passer le potentiel zeta de négatif en positif, les particules devenant progressivement plus positives aux taux de calcium soluble plus élevés. Au contraire, l'augmentation des taux de phosphate soluble rendait le potentiel zeta des particules de PCL nettement plus négatif. Ces résultats indiquent que l'addition de calcium soluble ou de phosphate soluble avait des effets spécifiques, probablement par leur liaison à la surface des particules de PCL. L'augmentation du taux d'agrégation dans les solutions de calcium soluble ne serait pas uniquement expliquée par les changements de potentiel zeta des particules.

**lait / calcium / phosphate / agrégation / potentiel zeta / force ionique**

## 1. INTRODUCTION

Milk is a complex food system containing milk-fat, proteins, minerals and carbohydrates (mainly lactose). Some components such as the lactose, the whey proteins and some of the mineral components are in true molecular solution. The casein proteins and much of the calcium and phosphate are associated with the colloidal particles (the casein micelles), whereas the milk-fat is found as complex emulsified droplets stabilized by a membrane composed of proteins and polar lipid components [20]. Skim milk contains about  $30 \text{ mmol}\cdot\text{L}^{-1}$  calcium and about  $20 \text{ mmol}\cdot\text{L}^{-1}$  inorganic phosphate of which about  $20 \text{ mmol}\cdot\text{L}^{-1}$  of calcium and  $10 \text{ mmol}\cdot\text{L}^{-1}$  of phosphate are associated with, and key structural elements of the casein micelles [10].

Many products, including dairy products can have their natural levels of calcium supplemented providing foods richer in dietary calcium. Most calcium additives are from non-food-derived sources such as calcium carbonates or calcium phosphates. A few

reports have indicated that it is possible to isolate calcium phosphate from dairy streams, such as cheese whey or milk permeate, and that these could be considered a natural food-derived source for calcium phosphate [7, 16]. A richer source of milk-derived calcium phosphate (MDCP) would be whey derived from acid casein or cottage cheese manufacture, as the calcium phosphate in milk is completely solubilized at the pH used in the manufacture of these products [4].

The MDCP can be isolated as a precipitated calcium phosphate material. However, the composition and properties of this material are poorly understood. Calcium phosphate is a general term encompassing a complex range of materials containing calcium and phosphate ions as basic components of their structures. The precipitation of calcium phosphate is complex and can undergo many phase changes [5, 14]. This study was aimed at examining the properties of MDCP when in suspension, and the factors affecting the stability of this calcium phosphate suspension.

## 2. MATERIALS AND METHODS

### 2.1. Materials

MDCP was obtained from Fonterra Cooperative Group, New Zealand (super fine milled ALAMIN<sup>TM</sup>). In the sample used, the average size of the particles was 2.9  $\mu\text{m}$ . Skim milk for permeate collection was purchased at a local supermarket. Hydroxyapatite (HAP) was obtained from Fluka Chemicals (Buchs, Germany). Samples of dicalcium phosphate dihydrate (DCPD) and amorphous calcium phosphate (ACP) were provided by Natalia Panova and Michael Mucalo (Waikato University, Hamilton, New Zealand). All other chemicals were obtained from Merck Chemicals (Darmstadt, Germany).

### 2.2. Preparation of MDCP stock suspensions

A 5% (w/w) suspension of the MDCP was prepared by adding the appropriate amount of the ALAMIN<sup>TM</sup> powder to purified water at ambient temperature (about 20 °C) and by stirring for 30 min. This suspension was considered to be the 3  $\mu\text{m}$  MDCP stock suspension. A fine fraction of MDCP was prepared by centrifugation of the 3  $\mu\text{m}$  stock solution. An aliquot of the 3  $\mu\text{m}$  stock calcium phosphate solution was placed in centrifuge tubes and centrifuged at low speed (2000 rpm) for a few seconds at 20 °C in a Sorvall Super T21 centrifuge with the associated Sorvall SL-50T rotor (Sorvall Products, Wilmington, Delaware, USA). This process removes the larger particles as a pellet and the smaller particles remain in the supernatant. The pellet was discarded, and the supernatant was measured for particle size using laser light scattering. The centrifugation process was repeated until the average particle size in the supernatant was about 0.5  $\mu\text{m}$ . The supernatant containing the 0.5  $\mu\text{m}$  sized calcium phosphate

particles was then centrifuged at 2000 rpm for 10 min to fully deposit the particles. The deposited particles were then resuspended in water to give a suspension with a concentration of about 5% (w/w) of the fine MDCP. This fine suspension was considered to be the 0.5  $\mu\text{m}$  MDCP stock suspension. Analysis of the 3 and 0.5  $\mu\text{m}$  MDCP particles indicated that their mineral composition was very similar.

### 2.3. Preparation of dispersing solutions

NaCl solutions (0.02–0.08  $\text{mol}\cdot\text{L}^{-1}$ ),  $\text{CaCl}_2$  solutions (1.25–5  $\text{mmol}\cdot\text{L}^{-1}$ ) or sodium phosphate solutions (0.625–5  $\text{mmol}\cdot\text{L}^{-1}$ , pH 7.0) were prepared by adding the appropriate quantity of NaCl,  $\text{CaCl}_2$  or  $\text{NaH}_2\text{PO}_4/\text{Na}_2\text{HPO}_4$ , respectively, to water and by stirring until they were dissolved. Milk permeate was obtained by the ultrafiltration of skim milk using a 10 000 Dalton (nominal) hollow fibre membrane cartridge and the associated pumping equipment (Amicon, Inc., Beverly, MA, USA). All solutions were used as prepared without pH measurement or adjustment.

### 2.4. Fourier transform infrared analysis

Fourier transform infrared (FTIR) spectra of the MDCP, HAP, ACP and DCPD were recorded using a Biorad Digilab FTS-40 FTIR (Digilab Division, Cambridge, MA, USA) using KBr disks that contained about 0.25% of the appropriate calcium phosphate in oven-dried KBr. Approximately 16 scans were acquired between 4000 and 700  $\text{cm}^{-1}$  at 4.0  $\text{cm}^{-1}$  resolution.

### 2.5. Particle sizing by laser light scattering

Particle size measurements using laser light scattering were performed using a Malvern Mastersizer 2000 (Malvern

Instruments Ltd., Malvern, Worcestershire, UK). A refractive index of 1.59 and particle absorption factor of 0.1 were used for all measurements. The sample was introduced into the cell until the desired obscuration (scattering intensity) was achieved. The average size obtained from the laser light scattering experiments is the volume to surface area mean, commonly referred to as the Sauter mean or the  $D[3,2]$  average size. The laser light scattering technique also reports the obscuration, which is the amount of light scattered from the particles.

### 2.6. Particle sizing by photon correlation spectroscopy

Particle size measurements by photon correlation spectroscopy (PCS) were made using a Malvern Zetasizer 4 instrument using the ZET5110 sizing cell (Malvern Instruments Ltd., Malvern, Worcestershire, UK). The samples of the MDCP were dispersed in the appropriate solutions to the concentrations that gave optimum scattering intensities. The temperature of the cell was controlled to better than  $\pm 0.2$  °C. Measurements of the dynamics of the scattered light were collected at a scattering angle of 90° only. Average diffusion coefficients were determined by the method of cumulants and translated into average particle diameters using the Stokes-Einstein relationship for spheres.

### 2.7. Measurement of the $\zeta$ -potential

A Malvern Zetasizer 4 instrument and the ZET5104 electrophoresis cell (Malvern Instruments Ltd., Malvern, Worcestershire, UK) were used for determining the  $\zeta$ -potential of the MDCP suspensions. The samples of the MDCP were dispersed in the appropriate solutions to the concentrations that gave optimum scattering intensities. The temperature of the cell was maintained at  $25 \pm 0.2$  °C. An applied voltage of 80 V and a modulation frequency of

250 Hz were used in all experiments. The electrophoretic mobility was experimentally determined, and the  $\zeta$ -potential was calculated from this electrophoretic mobility.

## 3. RESULTS AND DISCUSSION

Skim milk contains about  $30 \text{ mmol}\cdot\text{L}^{-1}$  calcium and about  $20 \text{ mmol}\cdot\text{L}^{-1}$  phosphate. At the natural pH of milk, this calcium and phosphate is distributed between the colloidal (casein micelles) and soluble phases of the milk. It is possible to isolate the calcium phosphate from milk as an insoluble calcium phosphate material from acidic whey solutions, cheese whey or milk/whey permeate [7, 16]. The pH reduction of milk to 4.6 will completely solubilize the calcium phosphate [4] and will precipitate the casein [17] leaving a whey solution containing all the milk minerals as well as the lactose and the whey proteins. Ultrafiltration of this acidic whey produces a retentate enriched in whey proteins, and a permeate containing the milk minerals and lactose. Increasing the pH of the permeate to about pH 7.0, along with heating will precipitate the calcium phosphate from the other soluble minerals and lactose, and this calcium phosphate can be washed, dried and milled to give the MDCP product. Although the product is predominantly calcium phosphate, there are some contaminants such as proteins (about 8%, mainly whey proteins that are transferred due to the inefficiencies of large-scale ultrafiltration), lactose (about 4%) and about 10% of other milk mineral components.

### 3.1. FTIR analysis of MDCP, HAP, ACP and DCPD

Figure 1 shows the infrared spectra obtained for the MDCP, with a comparison to those obtained for HAP, ACP and DCPD. There are detailed reports on the infrared spectra, including assignment of the major

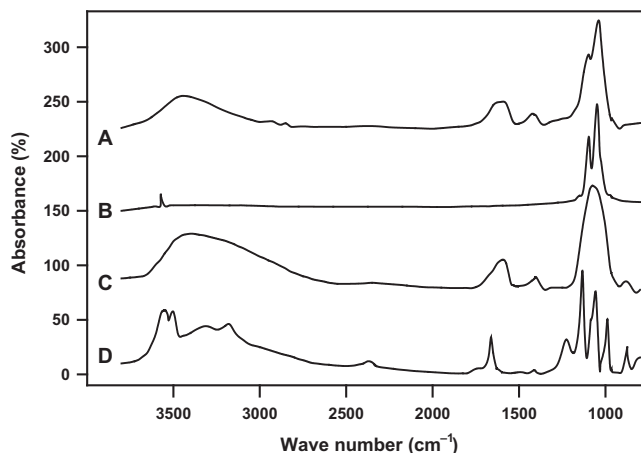


**Figure 1.** FTIR spectra for various calcium phosphate materials. (A) MDCP, (B) HAP, (C) ACP and (D) DCPD.

bands for HAP [1–3, 15], ACP [13, 15] and DCPD [18]. Overall, the infrared spectra obtained in the present study were comparable with the literature reports for these compounds. Hence, very general band assignments can be made. The HAP had a very weak band at  $3572\text{ cm}^{-1}$  which is likely to be due to the OH stretching mode. The MDCP, DCPD and ACP had a broad band from about  $3700\text{--}2500\text{ cm}^{-1}$  and a sharper band at about  $1600\text{ cm}^{-1}$ . The former can be assigned to the OH stretching and the latter to the OH bending modes of water. The series of bands from about  $1300\text{--}700\text{ cm}^{-1}$  can be assigned to the various P–O and P–O(H) stretching modes, although those at higher wave numbers (about  $1200\text{--}1300\text{ cm}^{-1}$ ) may be the P–O–H bending modes [15, 18].

From the FTIR spectra, it appears that the MDCP is composed of poorly crystalline HAP. However, it is also possible that MDCP has some ACP. This is consistent with the expectations as the rapid precipitation of calcium phosphate solutions under slightly alkaline conditions produces an insoluble solid with low crystallinity called

ACP [5, 6]. ACP can transform by a process of redissolving and reprecipitation to semi-crystalline solids such as DCPD and octacalcium phosphate (OCP), depending on the pH. The DCPD and OCP gradually take on the characteristics of HAP [14, 16]. Further characterization of the various phosphates could be made by obtaining  $^{31}\text{P}$  NMR spectra. When the information from NMR is combined with that from FTIR, a more conclusive characterization of the composition of the MDCP would be possible especially if the material is amorphous or poorly crystalline [8, 9, 19, 21].

### 3.2. Particle size changes of MDCP suspensions in water and milk permeate

The  $0.5$  and  $3\text{ }\mu\text{m}$  MDCP stock suspensions were dispersed in water and the size was measured at various time intervals without stirring. Figures 2A and 2B show the particle size distribution for the  $0.5$  and  $3\text{ }\mu\text{m}$  samples, respectively, on initial measurement (Figs. 2A(i) and 2B(i)), and after a period of 30 min (Figs. 2A(ii)

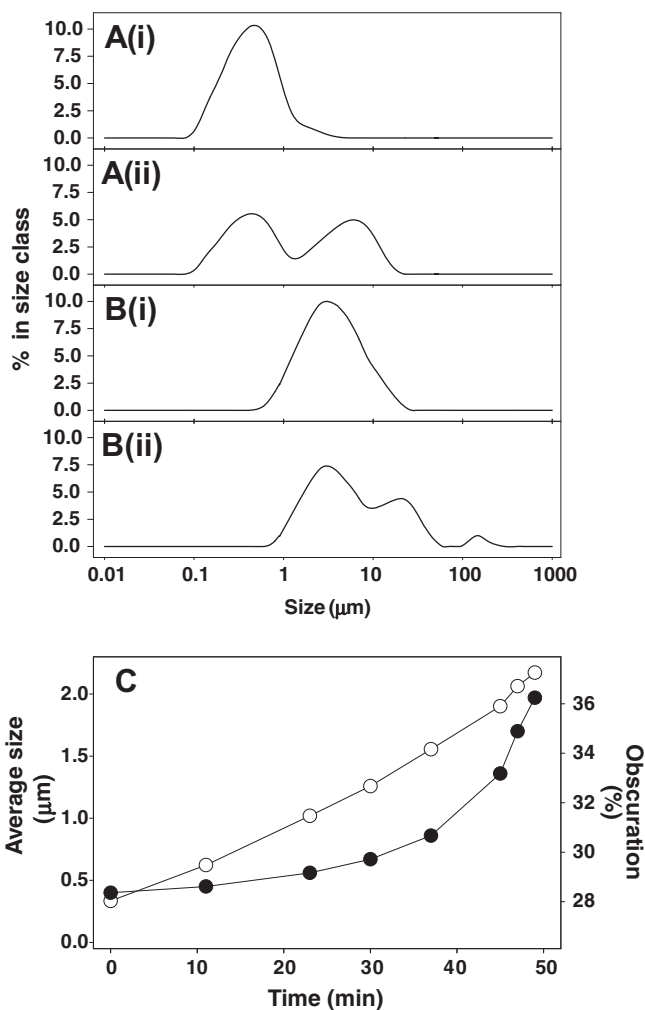


**Figure 2.** Particle size characterization of MDCP suspensions in water using laser light scattering. (A) MDCP with a 0.5  $\mu\text{m}$  average size. (i) Initial size distribution and (ii) size distribution after 30 min without mixing. (B) MDCP with a 3  $\mu\text{m}$  average size. (i) Initial size distribution and (ii) size distribution after 30 min without mixing. (C) Change in average size and obscuration for MDCP with a 0.5  $\mu\text{m}$  average size. ●, average size; ○, obscuration.

and 2B(ii)). In both cases, the initial size measurement showed an approximately normal size distribution with the 0.5  $\mu\text{m}$  sample having an average size of 0.45  $\mu\text{m}$ , and the 3  $\mu\text{m}$  sample having an average size

of 2.9  $\mu\text{m}$ . However, a measurement of the size after a time period of 30 min showed that the size distribution had changed markedly, with the distribution becoming multimodal due to the appearance of larger

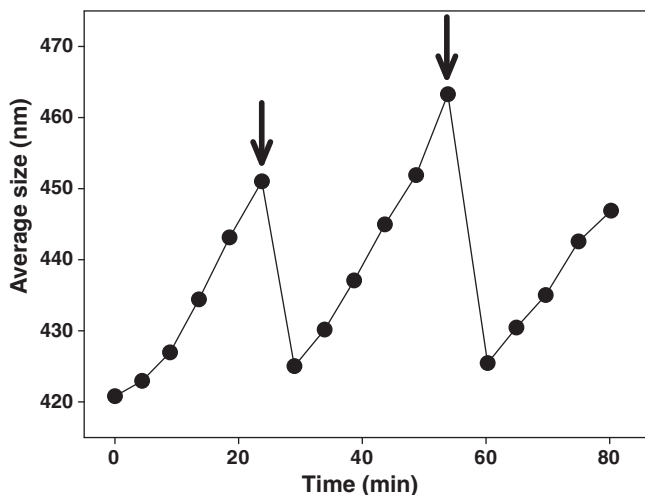


**Figure 3.** Changes in average size with time for the 0.5  $\mu\text{m}$  MDCP suspensions in water, as determined using PCS. The arrows indicate the point at which the sample was mixed.

size modes. When the sample was subsequently stirred, the average size and the size distribution returned to the initial state.

The effect of holding time on the average size for the 0.5  $\mu\text{m}$  sample can be clearly seen in Figure 2C. The average size increased almost exponentially with time from 0.4  $\mu\text{m}$  for the first measurement to about 2  $\mu\text{m}$  after about 50 min. As the scattering intensity of light from particles is proportional to (diameter)<sup>6</sup>, the amount of light scattered from the particles would be expected to increase during aggregation. The obscuration was found to increase with the time the sample was in the measuring cell supporting the observed increases in size (Fig. 2C).

All subsequent particle sizing measurements of the MDCP suspensions were performed using the PCS technique. The 3  $\mu\text{m}$  and the 0.5  $\mu\text{m}$  MDCP particles behaved similarly when in aqueous solution (Fig. 2); however, the 3  $\mu\text{m}$  particles were too large to allow accurate size changes to be monitored by PCS. Therefore, all subsequent experiments used the 0.5  $\mu\text{m}$

MDCP stock solution as these particles were in the ideal range for size measurements by PCS. Figure 3 shows the change in average size with time for the MDCP in water. As observed with laser light scattering, the average size increased progressively with time. However, gentle stirring returned the average size close to its initial level, and then the size started increasing again. These results indicate that the size is increasing due to the aggregation of the particles; however, the forces holding these aggregates together are very weak so that gentle agitation disrupted the aggregates and returned the size back to those of the initial primary particles.

For all subsequent experiments, the size is recorded as the change in size relative to the initial particle size. The rate of aggregation of the MDCP in water was markedly dependent on temperature (Fig. 4A). At 20  $^{\circ}\text{C}$ , the size increased only slowly with time so that after 60 min, the size was only about 10 nm larger than the initial size. As the temperature was increased, the rate of aggregation increased so that at 34  $^{\circ}\text{C}$ ,



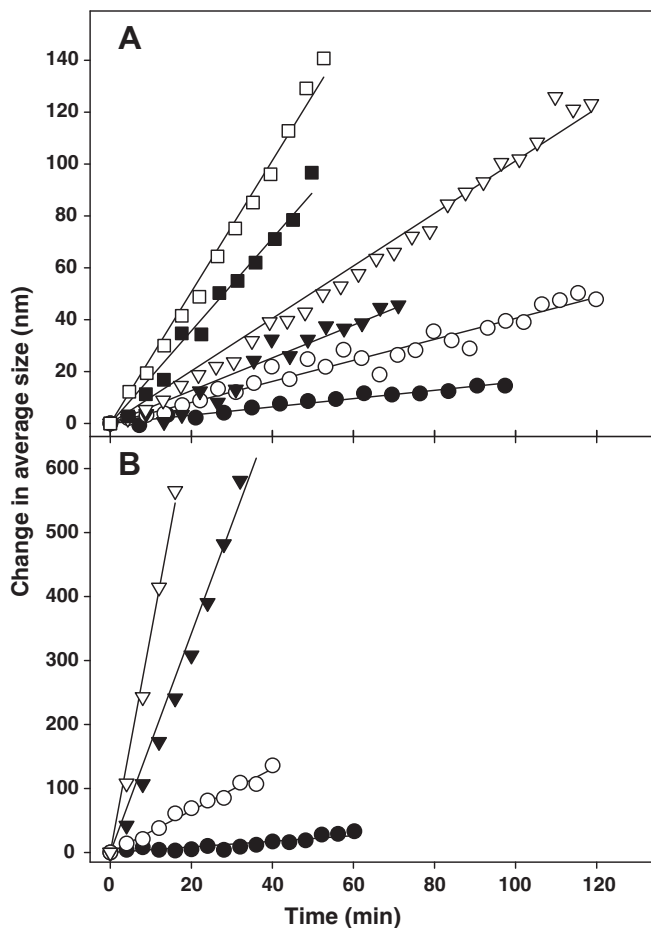


**Figure 4.** Effect of temperature on the changes in average size with time for the 0.5  $\mu\text{m}$  MDCP suspensions, as determined using PCS. (A) MDCP dispersed in water. Samples were held at temperatures of: ●, 20 °C; ○, 25 °C; ▼, 27 °C; ▽, 29 °C; ■, 32 °C; □, 34 °C. (B) MDCP dispersed in milk permeate. Samples were held at temperatures of: ●, 20 °C; ○, 22.5 °C; ▼, 25 °C; ▽, 30 °C.

the size after 60 min was about 150 nm larger than the initial size. When the MDCP was dispersed in milk permeate, a similar effect of temperature was observed, with a more rapid rate of aggregation at higher temperatures (Fig. 4B). However, at any equivalent temperature, the rate of aggregation in the milk permeate was markedly faster than in water. As an estimate of the difference in the rate of aggregation between the samples

dispersed in water and in milk permeate the temperature coefficient ( $Q_{10}$ ) was determined. The  $Q_{10}$  is a measure of the factor that a reaction rate increases for every 10 °C rise in temperature. The  $Q_{10}$  can be calculated using equation (1), where the rates of aggregation (in  $\text{nm}\cdot\text{min}^{-1}$ ) at each temperature were obtained from the slopes of the lines shown in Figure 4. For the MDCP in water, the  $Q_{10}$  was found to be

about 7.7 regardless of which two rates/temperatures were used for the calculation. For the MDCP in milk permeate, the  $Q_{10}$  was markedly higher when calculated from the aggregation rates at the lower temperatures than those calculated at the higher temperatures. The  $Q_{10}$  was about 77 when calculated using the rates from the 20 and 30 °C samples indicating that the rate of aggregation of MDCP was an order of magnitude faster in milk permeate than in water when the temperature was raised from 20 to 30 °C

$$Q_{10} = (R_2/R_1)^{(10/T_2-T_1)}. \quad (1)$$

Although there are no reported studies on the suspension properties of MDCP, there are studies on more specific calcium phosphate species, in particular HAP to which comparisons can be made. The MDCP has low suspension stability in water, forming weakly bound aggregates that can be redispersed by gentle agitation (Figs. 2–4). HAP nanoparticles have been reported to aggregate or agglomerate in aqueous suspensions to form microscale clusters, and this has created problems in the processing and the use of nanophase HAP-based materials [1, 3]. In fact, there have been extensive studies on the modification of the surface properties of HAP to improve its suspension stability [1–3, 11, 12].

In water, the effects of temperature on this aggregation may be simply due to an increased number of inter-particle encounters at higher temperatures. The rate at which particles will aggregate depends on the frequency at which the particles encounter each other and the probability that the thermal energy of the particles is sufficient to overcome the repulsive forces between the particles. In the non-agitated state used in these experiments, particle-particle encounters are solely a consequence of Brownian motion. As the mean kinetic energy of Brownian motion is proportional

to temperature, particles will exhibit increased Brownian motion at higher temperatures, therefore, an increased number of particle-particle encounters will occur and the aggregation rate will increase.

### 3.3. Particle size changes and $\zeta$ -potential of MDCP suspensions at 25 °C in solutions of different ionic strengths

Aqueous solutions of different ionic strengths were prepared by adding NaCl to water at concentration ranging from 0 to 0.08 mol·L<sup>-1</sup>. The MDCP was added to these solutions, and the particle size change with time at 25 °C was followed (Fig. 5A). From the slope of these curves, the rate of aggregation (in nm·min<sup>-1</sup>) was calculated (Fig. 5B). The rate of aggregation of the MDCP increased from about 0.5 to about 2 nm·min<sup>-1</sup> as the ionic strength increased from 0 to 0.08 mol·L<sup>-1</sup> (Fig. 5). Figure 5B also shows the change in  $\zeta$ -potential of the particles with ionic strength. The magnitude of the  $\zeta$ -potential decreased from about -9 to about -5.5 mV as the ionic strength increased from 0 to 0.08 mol·L<sup>-1</sup>.

Huang et al. [11] studied the effect of ionic strength on the  $\zeta$ -potential of HAP suspensions. They reported that the magnitude of the  $\zeta$ -potential increased slightly from about -13 to about -18 mV as the ionic strength increased from 0 to 0.01 mol·L<sup>-1</sup>, then decreased progressively with further increases in ionic strength so that the  $\zeta$ -potential at an ionic strength of 0.1 mol·L<sup>-1</sup> was about -4 mV. With the exception of the behaviour at ionic strengths < 0.01 mol·L<sup>-1</sup>, these values for the  $\zeta$ -potential of HAP and the effects of increasing ionic strength were comparable to those observed in this study for the MDCP (Fig. 5B).

The increased rate of aggregation of the MDCP suspensions when the ionic strength was increased (Fig. 5) could be explained

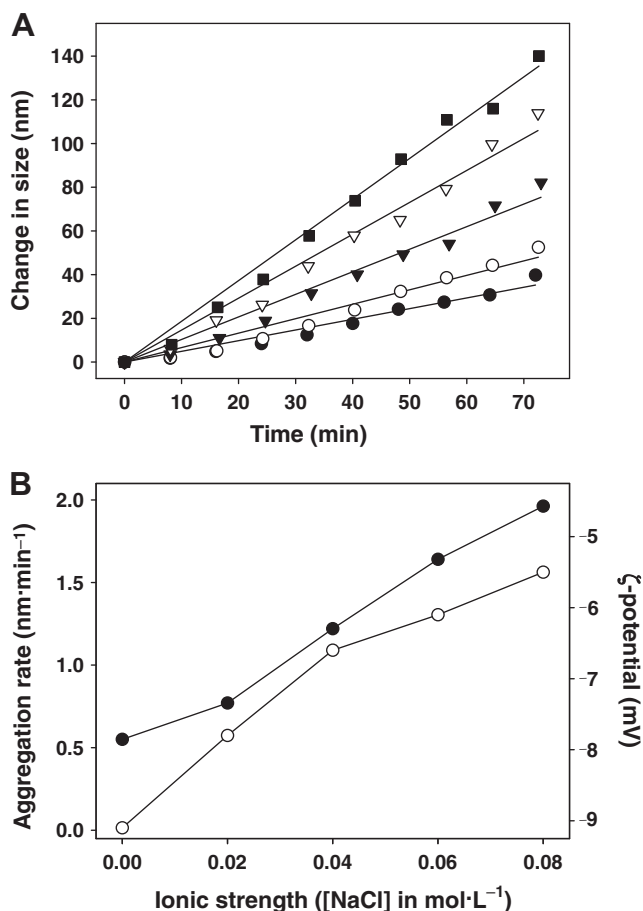


**Figure 5.** Effect of ionic strength (NaCl concentration) on the changes in average size with time for the 0.5  $\mu\text{m}$  MDPC suspensions at 25  $^{\circ}\text{C}$ , as determined using PCS. (A) MDPC dispersed in solutions of different ionic strengths. The samples were dispersed in solutions with NaCl concentration of: ●, 0  $\text{mol}\cdot\text{L}^{-1}$ ; ○, 0.02  $\text{mol}\cdot\text{L}^{-1}$ ; ▼, 0.04  $\text{mol}\cdot\text{L}^{-1}$ ; ▽, 0.06  $\text{mol}\cdot\text{L}^{-1}$ ; ■, 0.08  $\text{mol}\cdot\text{L}^{-1}$ . (B) Effect of ionic strength (NaCl concentration) on the rate of aggregation and  $\zeta$ -potential of MDPC suspensions. ●, rate of aggregation; ○,  $\zeta$ -potential.

by the effects of the increased electrolyte concentrations on the  $\zeta$ -potential of the suspended particles. In general, the colloidal stability of the particles can be described in terms of the DLVO theory [14, 20], which considers both the short range electrostatic interactions between particles through their electric double layers (usually

repulsive) and the longer range van der Waals electrodynamic interactions between the particles (usually attractive). The  $\zeta$ -potential gives an indication of the repulsive forces between the particles and how this is affected by changes to the suspending medium. Compared with stable colloidal materials, the MDPC suspensions have

low  $\zeta$ -potentials even when suspended in water, and this would account for the progressive aggregation when in suspension (Figs. 2–5). Increasing the ionic strength will compress the electrical double layer resulting in a decrease in the  $\zeta$ -potential and the electric repulsive forces between the particles. Therefore, the stability of the suspended particles is decreased by increased ionic strength and the aggregation rate would be increased as is observed (Fig. 5).

### 3.4. Particle size changes and $\zeta$ -potential of MDCP suspensions in water containing different levels of added soluble calcium or phosphate

Aqueous solutions with soluble calcium or phosphate levels at concentration ranging from 0 to 5 mmol·L<sup>-1</sup> were prepared, and the MDCP was added to these solutions. The particle size change with time at 25 °C was followed (Figs. 6A and 6B). From the slope of these curves, the rate of aggregation (in nm·min<sup>-1</sup>) was calculated (Fig. 6C). The rate of aggregation of the MDCP increased from about 0.5 to about 18 nm·min<sup>-1</sup> as the soluble calcium concentration was increased from 0 to 5 mmol·L<sup>-1</sup> (Fig. 6). The rate of aggregation of the MDCP in 5 mmol·L<sup>-1</sup> soluble calcium solutions was considerably higher than when suspended in 0.08 mol·L<sup>-1</sup> NaCl solution (Fig. 5) even though the latter has an ionic strength over five times that of the suspension in calcium solution. In contrast, the rate of aggregation in the phosphate solution decreased slightly from about 0.5 to about 0.3 nm·min<sup>-1</sup> as the soluble phosphate level was increased from 0 to 5 mmol·L<sup>-1</sup> (Fig. 6).

The changes in  $\zeta$ -potential of the MDCP particles with increasing soluble calcium or phosphate concentrations are shown in Figure 6C. The  $\zeta$ -potential of the particles in the water was about -9 mV. On addition of 1.25 mmol·L<sup>-1</sup> soluble calcium, the

$\zeta$ -potential of the particles changed from negative (about -9 mV) to positive (about +0.5 mV). As the level of soluble calcium was increased further, the  $\zeta$ -potential became more positive, increasing from about +0.5 to about +8 mV as the soluble calcium level increased from 1.25 to 5 mmol·L<sup>-1</sup>. In contrast, the  $\zeta$ -potential of the particles became more negative as the soluble phosphate level was increased, changing from about -9 to about -19 mV as the soluble phosphate level was increased from 0 to 5 mmol·L<sup>-1</sup> (Fig. 6C).

The results shown in Figure 6 suggest that the added calcium and phosphate are having more specific effects than the NaCl (Fig. 5), as these effects cannot be simply explained by the changes in ionic strength. As calcium has a much stronger affinity for phosphate than sodium, it is possible that the added soluble calcium adsorbs to the surface of the MDCP particles, initially neutralizing the negative charges on the particles at low calcium levels and then progressively producing positively charged particles at higher calcium levels. Similarly, the added soluble phosphate may adsorb to the surface of the calcium phosphate, producing more negatively charged particles as the level of phosphate increased. Zhu et al. [22] have shown that the  $\zeta$ -potential of biphasic calcium phosphate particles changed from negative to positive when low levels of soluble calcium were added to the suspension. At high levels of added soluble calcium ( $\geq 50$  mmol·L<sup>-1</sup>), the  $\zeta$ -potential plateaued at about +30 mV, compared to about -9 mV for the biphasic calcium phosphate suspensions in water. Zhu et al. [22] also showed that the  $\zeta$ -potential of the biphasic calcium phosphate became markedly more negative on the addition of soluble phosphate, changing from about -9 to about -35 mV as the level of soluble phosphate was increased from 0 to 10 mmol·L<sup>-1</sup>. Further, minor change in  $\zeta$ -potential was observed at higher soluble phosphate levels. These effects of

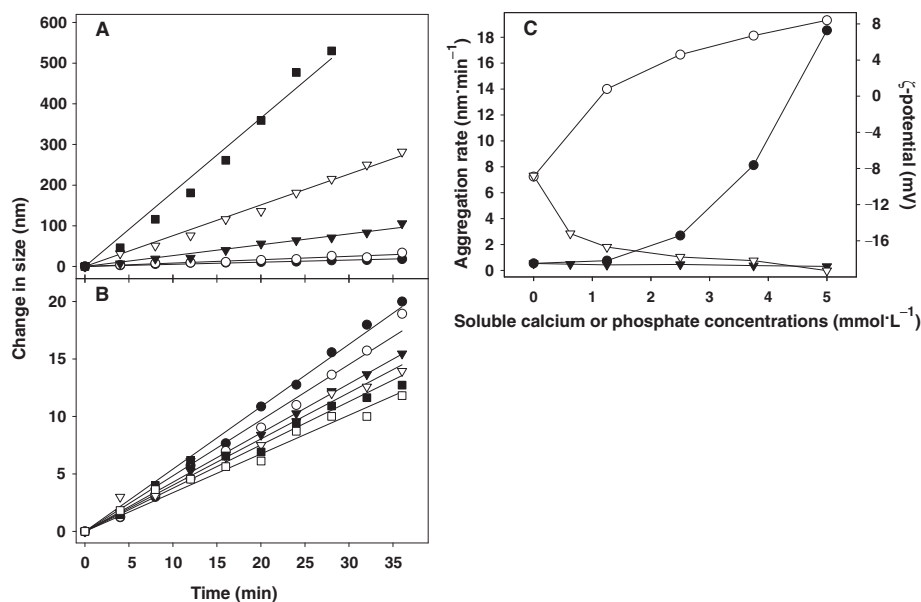


**Figure 6.** Effect of soluble calcium and soluble phosphate on the changes in average size with time for the 0.5  $\mu\text{m}$  MDCP suspensions at 25  $^{\circ}\text{C}$ , as determined using PCS. (A) MDCP dispersed in solutions of different soluble calcium levels. The soluble calcium levels were:  $\bullet$ , 0  $\text{mmol}\cdot\text{L}^{-1}$ ;  $\circ$ , 1.25  $\text{mmol}\cdot\text{L}^{-1}$ ;  $\blacktriangledown$ , 2.5  $\text{mmol}\cdot\text{L}^{-1}$ ;  $\nabla$ , 3.75  $\text{mmol}\cdot\text{L}^{-1}$ ;  $\blacksquare$ , 5  $\text{mmol}\cdot\text{L}^{-1}$ . (B) MDCP dispersed in solutions of different soluble phosphate levels. The soluble phosphate levels were:  $\bullet$ , 0  $\text{mmol}\cdot\text{L}^{-1}$ ;  $\circ$ , 0.625  $\text{mmol}\cdot\text{L}^{-1}$ ;  $\blacktriangledown$ , 1.25  $\text{mmol}\cdot\text{L}^{-1}$ ;  $\nabla$ , 2.5  $\text{mmol}\cdot\text{L}^{-1}$ ;  $\blacksquare$ , 3.75  $\text{mmol}\cdot\text{L}^{-1}$ ;  $\square$ , 5  $\text{mmol}\cdot\text{L}^{-1}$ . (C) Effect of soluble calcium and soluble phosphate on the rate of aggregation and  $\zeta$ -potential of MDCP suspensions.  $\bullet$ , rate of aggregation in soluble calcium solutions;  $\circ$ ,  $\zeta$ -potential in soluble calcium solutions;  $\blacktriangledown$ , rate of aggregation in soluble phosphate solutions;  $\nabla$ ,  $\zeta$ -potential in soluble phosphate solutions.

soluble calcium or soluble phosphate on the  $\zeta$ -potential of the biphasic calcium phosphate suspensions were ascribed to the adsorption of the added calcium or phosphate onto the particles, with saturation in adsorption occurring at calcium or phosphate concentrations where the  $\zeta$ -potential plateaued [22].

Although the stability of the MDCP in NaCl (Fig. 5) and soluble phosphate (Fig. 6) solutions can be explained by simple changes to the  $\zeta$ -potential of the particles, the results for the suspension in soluble calcium solutions (Fig. 6) indicate that the  $\zeta$ -potential on the MDCP is not

the sole determinant of the stability of the particles. For example, when soluble calcium was added to the suspensions, the lowest magnitude of  $\zeta$ -potential (i.e., closest to 0) was observed at a calcium level of 1.25  $\text{mmol}\cdot\text{L}^{-1}$ , yet the rate of aggregation of the particles at this calcium level was lower than in samples with higher soluble calcium levels even though the particles were more highly charged at these higher calcium levels (Fig. 6). One possible explanation is that the adsorption of calcium alters the properties of the surface of the calcium phosphate particles making them more prone to interaction so that, during

Brownian motion, a greater proportion of the particle contacts lead to aggregation than when the particles are suspended in water or soluble phosphate solutions. Alternatively, it is possible that the added calcium can act as a bridging agent between particles through electrostatic interactions, thereby increasing the rate of aggregation when higher levels of calcium are added. Clearly the aggregation of the MDCP particles when suspended in milk permeate is determined by the ionic strength of the solution as well as the specific effects of the soluble calcium and phosphate, and possibly other milk minerals.

**Acknowledgements:** Drs. M. Mucalo, N. Panova and A. Rogers are thanked for useful discussions and comments. This work was supported by funding from the New Zealand Foundation for Research Science and Technology (Contract No. DRIX0701).

## REFERENCES

- [1] Borum L., Wilson O.C., Surface modification of hydroxyapatite. Part II. Silica, *Biomaterials* 24 (2003) 3681–3688.
- [2] Borum-Nicholas L., Wilson O.C., Surface modification of hydroxyapatite. Part I. Dodecyl alcohol, *Biomaterials* 24 (2003) 3671–3679.
- [3] Choi H.W., Lee H.J., Kim K.J., Kim H.M., Lee S.C., Surface modification of hydroxyapatite nanocrystals by grafting polymers containing phosphonic acid groups, *J. Colloid Interface Sci.* 304 (2006) 277–281.
- [4] Dalgleish D.G., Law A.J.R., pH-induced dissociation of bovine casein micelles. II. Mineral solubilization and its relation to casein release, *J. Dairy Res.* 56 (1989) 727–735.
- [5] Eanes E.D., Posner A.S., Kinetics and mechanism of conversion of noncrystalline calcium phosphate to crystalline hydroxyapatite, *Trans. N. Y. Acad. Sci.* 28 (1965) 233–241.
- [6] Feenstra T.P., Debruyen P.L., Light scattering studies on solutions containing calcium phosphates, *J. Colloid Interface Sci.* 73 (1980) 431–437.
- [7] Harju M., Milk sugars and minerals as ingredients, *Int. J. Dairy Technol.* 54 (2001) 61–63.
- [8] Heimann R.B., Tran H.V., Hartmann P., Laser-Raman and nuclear magnetic resonance (NMR) studies on plasma-sprayed hydroxyapatite coatings: influence of bioinert bond coats on phase composition and resorption kinetics in simulated body fluid, *Materialwiss. Werkstofftech.* 34 (2003) 1163–1169.
- [9] Holt C., Wahlgren N.M., Drakenberg T., Ability of a  $\beta$ -casein phosphopeptide to modulate the precipitation of calcium phosphate by forming amorphous dicalcium phosphate nanoclusters, *Biochem. J.* 314 (1996) 1035–1039.
- [10] Horne D.S., Casein micelle structure: models and muddles, *Curr. Opin. Colloid Interface Sci.* 11 (2006) 148–153.
- [11] Huang F.Z., Shen Y.H., Xie A.J., Zhu J.M., Zhang C.Y., Li S.K., Zhu J., Study on synthesis and properties of hydroxyapatite nanorods and its complex containing biopolymer, *J. Mater. Sci.* 42 (2007) 8599–8605.
- [12] Lee S.C., Choi H.W., Lee H.J., Kim K.J., Chang J.H., Kim S.Y., Choi J., Oh K.S., Jeong Y.K., In-situ synthesis of reactive hydroxyapatite nano-crystals for a novel approach of surface grafting polymerization, *J. Mater. Chem.* 17 (2007) 174–180.
- [13] Li Y., Wiliana T., Tam K.C., Synthesis of amorphous calcium phosphate using various types of cyclodextrins, *Mater. Res. Bull.* 42 (2007) 820–827.
- [14] Liu Y., Nancollas G.H., Crystallization and colloidal stability of calcium phosphate phases, *J. Phys. Chem. B* 101 (1997) 3464–3468.
- [15] Mitchell P.C.H., Parker S.F., Simkiss J., Simmons J., Taylor M.G., Hydrated sites in biogenic amorphous calcium phosphates: an infrared, Raman, and inelastic neutron scattering study, *J. Inorg. Biochem.* 62 (1996) 183–197.
- [16] Spanos N., Patis A., Kanellopoulou D., Andritsos N., Koutsoukos P.G., Precipitation of calcium phosphate from simulated milk ultrafiltrate solutions, *Cryst. Growth Des.* 7 (2007) 25–29.
- [17] Swaisgood H.E., Chemistry of milk protein, in: Fox P.F. (Ed.), *Developments in Dairy*

- Chemistry, vol. 1: Proteins, Elsevier Applied Science, London, UK, 1982, pp. 1–59.
- [18] Trpkovska M., Soptrajanov B., Malkov P., FTIR reinvestigation of the spectra of synthetic brushite and its partially deuterated analogues, *J. Mol. Struct.* 481 (1999) 661–666.
- [19] Tseng Y.H., Tsai Y.L., Tsai T.W.T., Chao J.C.H., Lin C.P., Huang S.H., Mou C.Y., Chan J.C.C., Characterization of the phosphate units in rat dentin by solid-state NMR spectroscopy, *Chem. Mat.* 19 (2007) 6088–6094.
- [20] Walstra P., Jenness R., *Dairy Chemistry and Physics*, John Wiley and Sons, New York, USA, 1984.
- [21] Wang L.J., Nancollas G.H., Calcium orthophosphates: crystallization and dissolution, *Chem. Rev.* 108 (2008) 4628–4669.
- [22] Zhu X.D., Fan H.S., Li D.X., Xiao Y.M., Zhang X.D., Protein adsorption and zeta potentials of a biphasic calcium phosphate ceramic under various conditions, *J. Biomed. Mater. Res. B Appl. Biomater.* 82B (2007) 65–73.